Magn Reson Med Sci 2020; 19; 154–158
doi:10.2463/mrms.tn.2018-0168
Published Online: May 30, 2019

TECHNICAL NOTE

Comparison of Silent Navigator Waveform Generation Methods

Yuji Iwadate[1*], Atsushi Nozaki[1], Yoshinobu Nunokawa[2], Shigeo Okuda[3], Hiroyuki Kabasawa[1], and Masahiro Jinzaki[3]

The silent navigator technique utilizes a non-selective excitation and an appropriate respiratory waveform generation method is necessary for an accurate motion detection. We compared three methods for silent navigator waveform generation. The profile generation method with coil selection (prof-selection) resulted in a high cross correlation with bellows signals and a large respiration amplitude. The prof-selection method should be used for silent navigator waveform generation.

Keywords: *abdominal imaging, navigator, silent magnetic resonance imaging, respiratory motion*

Introduction

Respiratory motion is a major limiting factor of abdominal MRI, especially when breath-hold compliance is difficult for a patient. A respiratory navigator echo technique[1] enables free-breathing abdominal MRI with minimal motion artifacts by synchronizing data sampling with respiratory motion. The navigator echo technique provides a simpler workflow than bellows because it does not need placement of an extra device on the subject. Also, respiratory triggering with navigator echo can provide superior image quality to bellows for the direct detection of internal organ motion.[2] The pencil-beam excitation technique[3,4] is commonly used in navigated abdominal MRI, but its rapidly switched high amplitude magnetic field gradients generate high levels of acoustic noise. The large acoustic noise causes not only simple annoyance and verbal communication difficulties but also causes potential hearing damage to a patient.[5]

Recently, a silent navigator technique was developed for silent respiratory-triggered MRI.[6] It utilizes a non-selective hard excitation radiofrequency (RF) pulse without gradient pulses during excitation and enables a remarkable reduction of acoustic noise. This non-selective excitation results in signal mixture from moving organs (e.g. liver) and static tissues (e.g. muscle on the back), whereas the conventional pencil-beam navigator excites the targeted moving liver by design. Therefore, an appropriate respiratory navigator waveform generation method is necessary for an accurate motion detection in the silent navigator scans.

The purpose of this study was to compare three silent-navigator waveform generation methods and to select the most suitable one for an accurate motion detection in respiratory navigated MRI.

[1]Global MR Applications and Workflow, GE Healthcare Japan, 4-7-127 Asahigaoka, Hino, Tokyo 191-8503, Japan
[2]Office of Radiation Technology, Keio University Hospital, Tokyo, Japan
[3]Department of Radiology, Keio University School of Medicine, Tokyo, Japan
*Corresponding author, Phone: +81-42-585-3453, Fax: +81-42-585-5725, E-mail: yuji.iwadate@ge.com

Received: December 11, 2018 | Accepted: April 4, 2019

Materials and Methods

Pulse sequence and navigator waveform generation

The silent navigator sequence has been previously described.[6] In short, it uses a non-selective hard RF pulse to avoid high levels of acoustic noise, which resulted in whole volume excitation. Dephasing and read-out gradient pulses in the superior–inferior direction follows the excitation for gradient echo acquisition. The slew rate for the read-out is derated compared with the conventional navigator to reduce acoustic noise.

The following three navigator waveform generation methods were compared using the same raw silent navigator echo data. These three methods are outlined in Fig. 1.

Motion correction using coil arrays (MOCCA)

The cross-correlation coefficient was calculated between the reference and each navigator data in *k*-space. The signals from the multi-coil elements were not combined before the correlation coefficient computation in order to make use of the differences in motion sensitivity among coil elements. The reference was chosen so that it would maximize the averaged correlation coefficient with all other data sets. A detailed description is given in the article Hu et al.[7]

Profile creation with all coil elements (prof-all)

A displacement was calculated after navigator signal profile creation in image space. The *k*-space navigator data

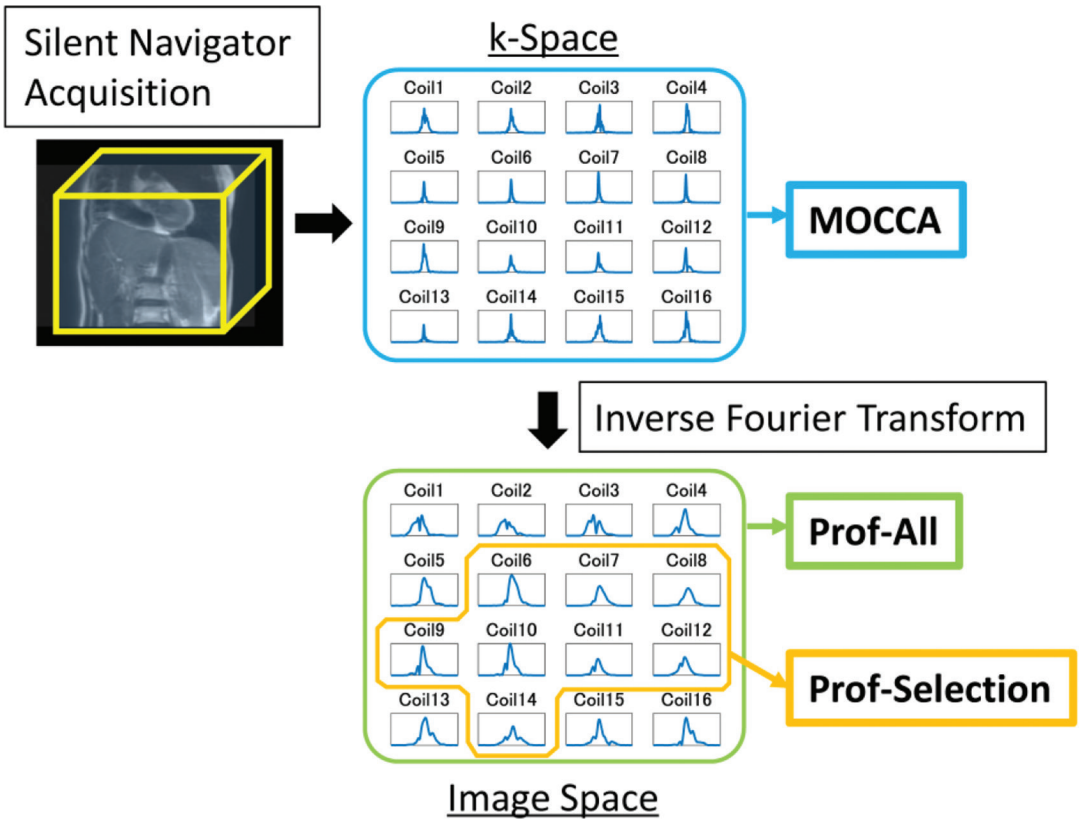

Fig. 1 Outline of three silent navigator waveform generation methods. Silent navigator signals acquired with non-selective excitation were received with a multi-coil array. MOCCA used *k*-space signals from all channels for calculation of cross correlation coefficients. The prof-all and prof-selection methods performed inverse Fourier transform to create navigator profiles in the image domain. The prof-all method combined all-channel signals whereas the prof-selection method selected coil elements using frequency analysis. MOCCA, motion correction using coil arrays; prof-all, profile creation with all coil elements; prof-selection, profile creation with selected coil elements.

were inverse-Fourier transformed into the image domain per each coil element, and image space data from all coil elements were combined to produce the final profile. A displacement between the reference (the first navigator data) and each profile was calculated using the least-squares error method.[8]

Profile creation with selected coil elements (prof-selection)

This method was identical to the prof-all method except that the coil selection was performed before the signal combination to extract signals sensitive to respiratory motion. Coil selection was conducted on the assumption that the respiratory motion occurs with the frequency from 0.1 to 0.5 Hz (corresponding to the cycle from 2 to 10 s) and that suitable coil signals have a peak within this range in the temporal frequency domain. For frequency analysis, the signals were extracted from the *k*-space position which provided the maximum signal intensity in the first acquisition, and this signal extraction was repeated for all coil elements. The signals were then Fourier transformed into the temporal frequency domain. After the signals in the frequency domain were normalized by the signal at 0 Hz per each coil, a half of the coil elements with the high signal peaks from 0.1 to 0.5 Hz in absolute value were selected. An example of different coil sensitivities to respiratory motion is shown in Fig. 2.

MR experiments

With Institutional Review Board approval, silent navigator scans were performed on seven healthy volunteers (four men, three women) using a 1.5T MR450w imaging system (GE Healthcare, Waukesha, WI, USA) and a 16-channel phased array coil. Silent navigator signals were obtained with 500-mm length and 256 readout points in the superior–inferior direction. Data was acquired in 10 s with repetition time of 100 ms (100 repetitions). Flip angle was 1°. A respiratory bellows was placed around a subject's abdomen and the bellows signal was recorded for comparison.

Data analysis

Navigator signal evaluation was performed by calculating Pearson's correlation coefficients between the bellows signals and the displacement values calculated with three different methods described above. All 100 navigator displacement values were used for calculation of the coefficient with the corresponding bellows signals acquired simultaneously in 10 s. For prof-all and prof-selection methods, a

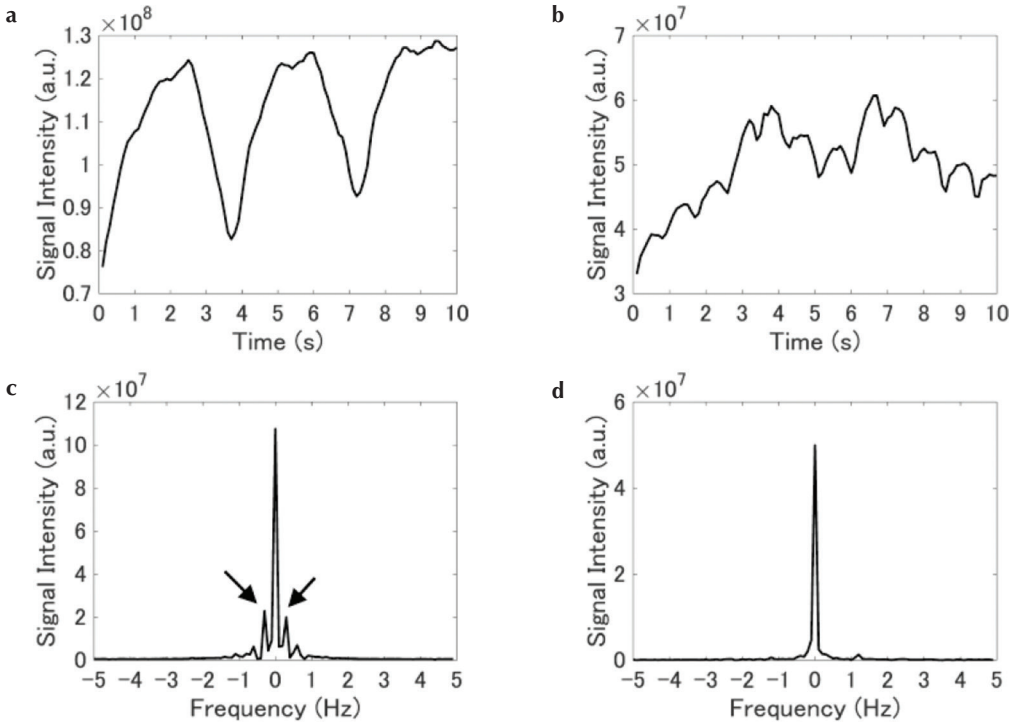

Fig. 2 Example of different coil sensitivities to respiratory motion. (**a** and **b**) Raw navigator signals from different two coil elements. (**c** and **d**) Fourier transformed data in the time domain. Spectra in (**c**) and (**d**) are generated from (**a**) and (**b**), respectively. The waveform in (**a**) reflects respiratory motion well, and resultant spectrum in (**c**) has obvious peaks from 0.1 to 0.5 Hz in absolute value (arrows).

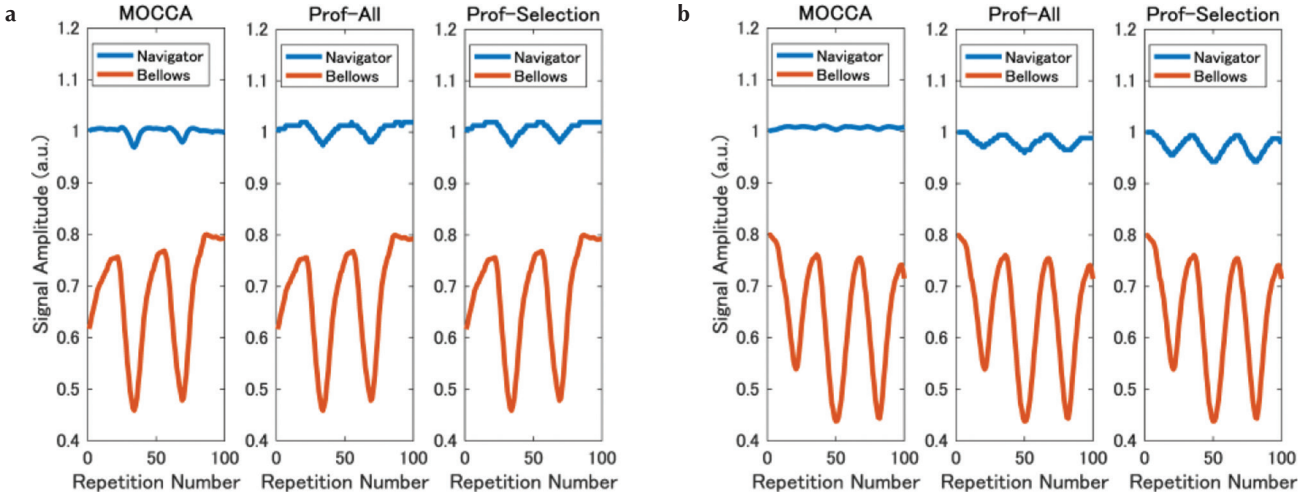

Fig. 3 Examples of navigator waveforms of MOCCA, prof-all and prof-selection. Bellows signals are also shown. Data are from volunteers 4 (**a**) and 5 (**b**). MOCCA, motion correction using coil arrays; prof-all, profile creation with all coil elements; prof-selection, profile creation with selected coil elements.

respiratory amplitude was also measured by calculating the absolute difference between the maximum and minimum displacement values.

Results

Figure 3 shows two examples of respiratory waveforms generated with the three methods. For volunteer 4 (Fig. 3a), the correlation coefficients between the bellows and the navigator waveforms were >0.7 with all three methods, but a flat portion was observed in every respiratory cycle with MOCCA method whereas the bellows signal did not show such characteristics. For volunteer 5 (Fig. 3b), MOCCA showed no correlation (correlation coefficient = 0.006, Vol. 5 in Fig. 4) with the bellows. Also, prof-selection had larger respiratory amplitude than prof-all.

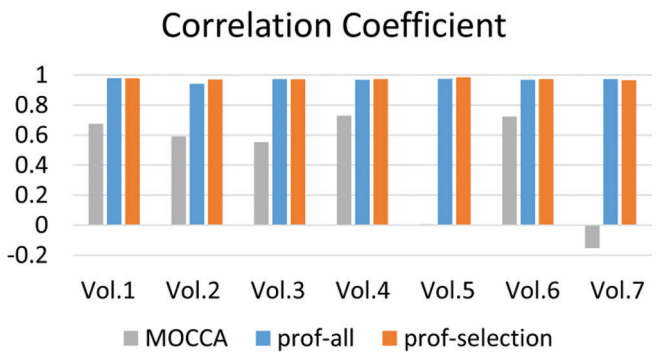

Fig. 4 Correlation coefficients between the bellows signals and the navigator displacements calculated from the three different methods for seven volunteers. Note that the value of MOCCA is 0.006 for volunteer 5 and not recognizable in the graph. MOCCA, motion correction using coil arrays; prof-all, profile creation with all coil elements; prof-selection, profile creation with selected coil elements; Vol, volunteers.

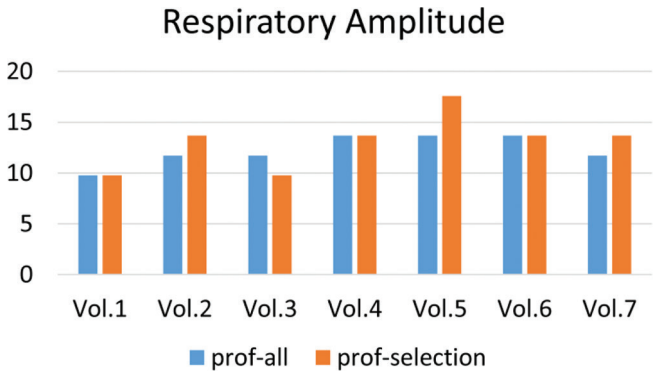

Fig. 5 Respiratory amplitudes calculated from waveforms with the prof-all and prof-selection methods for seven volunteers. prof-all, profile creation with all coil elements; prof-selection, profile creation with selected coil elements; Vol, volunteers.

Figure 4 shows the correlation coefficients between the bellows signal and each navigator displacement. All correlation coefficients for both prof-all and prof-selection were >0.9, showing an excellent correlation between the bellows and the navigator waveforms. On the other hand, the correlation coefficient was >0.7 for only two subjects with MOCCA. Furthermore, a negative correlation was observed in one subject (Vol. 7).

Figure 5 shows the respiratory amplitude detected with the prof-all and prof-selection methods. The amplitude of prof-selection was larger than that of prof-all for three subjects, and smaller for one subject.

Discussion

This study compared three silent navigator waveform generation methods by computing cross-correlation coefficients with the bellows signals and measuring the respiratory amplitude. One method generated the waveforms directly from the *k*-space data (MOCCA), and the other two used the profile displacements after inverse-Fourier transform of *k*-space data into the image domain (prof-all and prof-selection). The prof-selection method had a good correlation with the bellows and a large respiratory amplitude.

The correlation coefficients between the bellows signals and the navigator displacement values tended to be low with MOCCA method. Also, a negative correlation was observed in one volunteer data probably because the reference was acquired at end-inspiration whereas it was acquired at end-expiration for the other subjects. These results imply that a direct motion detection from *k*-space data is not robust because each *k*-space signal includes information from the whole area where the coil element itself is sensitive within the FOV. This effect could be increased in the silent navigator with the whole volume excitation whereas the original MOCCA processing was applied to the slice-selective self-gating sequence.[7] The inverse Fourier transform successfully extracted the signals along the frequency encoding direction (the superior–inferior direction in our experiments) resulting in an effective motion detection in this direction and a larger correlation with the bellows for prof-all and prof-selection methods. Also, the respiration phase can be deduced directly from the displacement value; inferior and superior positions imply end-inspiration and end-expiration, respectively.

Between the two profile creation methods, the waveforms of prof-all tended to have a smaller respiratory amplitude compared with those of prof-selection. The signals from the static tissues might have affected the motion detection in the prof-all method. The prof-selection method reduces these static signals by excluding coil element signals which does not have much sensitivity to the respiratory motion. Inter-individual variation of the navigator waveforms could be caused by body shape, especially the amount of subcutaneous fat whose signal disrupts internal organ motion detection with the silent navigator echo.

Respiratory triggered imaging was performed with the prof-selection method in the previous study, resulting in image quality improvement compared with free breathing non-triggered scan.[6] This prof-selection technique can also be applied to the conventional pencil-beam navigator scan where the finite excitation period can cause a signal excitation outside the region of interest resulting in a motion detection error.[9] In this study, we chose half of the coil elements with the high signal peaks from 0.1 to 0.5 Hz in the temporal domain. The frequency range and the number or percentage of selected coil elements should be verified and/or optimized in the clinical conditions.

There are several limitations in this study. We did not compare the actual respiratory gated/triggered images with these navigator waveform generation methods. However, it is obvious that the flatter waveform of MOCCA with a smaller correlation to the bellows signals makes it more difficult to distinguish expiration and inspiration states and may produce severe motion artifacts in the final images. Also, a smaller respiratory amplitude in the navigator signals can

lead to the acceptance of undesirable data during respiratory gating/triggering imaging due to an underestimation of motion, and this could also result in motion artifacts and blurring, as can be seen in the non-triggered images in the previous study.[6] Another limitation is that we only performed experiments on seven healthy volunteers and therefore a clinical evaluation with larger number of subjects is required in future.

Conclusion

In this study, we compared three silent navigator waveform generation methods. The prof-selection method had a good correlation with bellows and a large respiratory amplitude. This method should be used for silent navigator waveform generation.

Acknowledgment

The authors thank Peng Lai for useful technical discussion and Takako Kurimoto for English editing.

Conflicts of Interest

Authors Yuji Iwadate, Atsushi Nozaki, and Hiroyuki Kabasawa are employees of GE Healthcare. Shigeo Okuda and Masahiro Jinzaki received research funding from GE Healthcare. Yoshinobu Nunokawa declares no conflict of interest associated with this manuscript.

References

1. Wang Y, Rossman PJ, Grimm RC, Riederer SJ, Ehman RL. Navigator-echo-based real-time respiratory gating and triggering for reduction of respiration effects in three-dimensional coronary MR angiography. Radiology 1996; 198:55–60.
2. Matsunaga K, Ogasawara G, Tsukano M, Iwadate Y, Inoue Y. Usefulness of the navigator-echo triggering technique for free-breathing three-dimensional magnetic resonance cholangiopancreatography. Magn Reson Imaging. 2013; 31:396–400.
3. Pauly J, Nishimura D, Macovski A. A k-space analysis of small-tip-angle excitation. J Magn Reson 1989; 81:43–56.
4. Hardy CJ, Cline HE. Broadband nuclear magnetic resonance pulses with two-dimensional spatial selectivity. J Appl Phys 1989; 66:1513–1516.
5. McJury M, Shellock FG. Auditory noise associated with MR procedures: a review. J Magn Reson Imaging 2000; 12:37–45.
6. Iwadate Y, Nozaki A, Nunokawa Y, Okuda S, Jinzaki M, Kabasawa H. Silent navigator-triggered silent MRI of the abdomen. Magn Reson Med 2018; 79:2170–2175.
7. Hu P, Hong S, Moghari MH, et al. Motion correction using coil arrays (MOCCA) for free-breathing cardiac cine MRI. Magn Reson Med 2011; 66:467–475.
8. Wang Y, Grimm RC, Felmlee JP, Riederer SJ, Ehman RL. Algorithms for extracting motion information from navigator echoes. Magn Reson Med 1996; 36:117–123.
9. Iwadate Y, Miyoshi K, Kabasawa H. Motion detection improvement of a pencil-beam navigator echo using a gradient reversal technique. Magn Reson Imaging 2015; 33:1168–1172.